China Ocean Eng., 2020, Vol. 34, No. 3, P. 314–327
DOI: https://doi.org/10.1007/s13344-020-0029-1, ISSN 0890-5487
http://www.chinaoceanengin.cn/ E-mail: coe@nhri.cn

MPS Method for Interaction Between Solitary Waves and Submerged Horizontal Plate

XU Yan-zhang, ZHAO Wei-wen, WAN De-cheng*

Computational Marine Hydrodynamics Lab (CMHL), State Key Laboratory of Ocean Engineering, School of Naval Architecture, Ocean and Civil Engineering, Shanghai Jiao Tong University, Shanghai 200240, China

Received October 25, 2019; revised January 4, 2020; accepted February 15, 2020

Abstract

The interaction between structure and wave is a typical phenomenon in naval architecture and ocean engineering. In this paper, numerical simulation is carried out to study the interaction between a two-dimensional submerged, fixed, horizontal rigid plate and solitary wave with our in-house meshless particle CFD solver MLParticle-SJTU. First, the in-house CFD solver is verified by experimental results conducted at the State Key Laboratory of Coastal and Offshore Engineering, Dalian University of Technology. During the verification, the plate is submerged under water and the solitary wave with a given amplitude is generated by a piston-type wave maker. Free surface elevation of the wave and the pressure impacting on the plate is recorded and compared with experimental data respectively. The predicted pressure and surface elevation agree well with the experimental results. Then in order to further investigate factors affecting wave-structure interaction, wave height, submerged depth and plate length are analyzed.

Key words: MPS method, MLParticle-SJTU solver, solitary waves, submerged horizontal plate, wave-plate interaction

Citation: Xu, Y. Z., Zhao, W. W., Wan, D. C., 2020. MPS method for interaction between solitary waves and submerged horizontal plate. China Ocean Eng., 34(3): 314–327, doi: https://doi.org/10.1007/s13344-020-0029-1

1 Introduction

The wave interaction is a particularly topical issue in the field of naval architecture and ocean engineering. The plate structure, such as the pier or a very large floating structure (VLFS), will suffer huge wave-induced loads which will challenge the safety and manipulation of the structure, while the plate in return influences the evolution of the wave. This issue is always one of the research hotspots and a lot of studies have been done regarding this problem including wave-induced pressure impacting on structures, influence of plate on the fluid field's evolution, flexible structures interaction with the wave and so on.

In general, this problem can be addressed with three kinds of methods namely experimental, numerical and empirical method respectively. Anastasiou and Shih (1992) dealt with the uplift loading induced by regular and irregular water wave on the underside of platform decks in shallow and intermediate water depths. Hayatdavoodi et al. (2014) researched solitary wave-induced forces on a two-dimensional model of a coastal bridge by conducting laboratory experiments and performing CFD computations. Irajpanah (1983) simulated the impact of the wave on a horizontal platform and analyzed the wave-induced pressure at the bottom of the deck. Greco et al. (2009) implemented the boundary element method (BEM) to investigate the coupling between the motion of a VLFS and the bottom slamming force. Seiffert et al. (2014) analyzed the wave pressure on a flat plate under the solitary wave based on the finite-volume method (FVM) with the help of the open source computational fluid dynamics (CFD) platform-OpenFOAM. Nelli et al. (2017) focused on the reflection and transmission of regular water waves by a thin floating plate.

The problems in the naval architecture and ocean engineering can be characterized by the free surface, the wave break or rolling, or violent flows, which requires extra treatments on tracking the boundaries of the water surface. Although the mesh-based methods are effective in the simulation of fluid evolution, they may still suffer from some difficulties and require complex strategies such as the adjustment or regeneration of mesh while tracking the complex boundaries. However, some newly emerged mesh-free methods can exactly overcome the difficulties regarding the

Foundation item: the National Natural Science Foundation of China (Grant Nos. 51909160 and 51879159), the National Key Research and Development Program of China (Grant Nos. 2019YFB1704200 and 2019YFC0312400), Chang Jiang Scholars Program (Grant No. T2014099), Shanghai Excellent Academic Leaders Program (Grant No. 17XD1402300), and Innovative Special Project of Numerical Tank of Ministry of Industry and Information Technology of China (Grant No. 2016-23/09).

*Corresponding author. E-mail: dcwan@sjtu.edu.cn

mesh-based method owing to their Lagrangian property. The smoothed particle hydrodynamics (SPH) and the moving particle semi-implicit (MPS) method are two typical particle-based mesh-free methods. SPH (Smoothed Particle Hydrodynamics) proposed by Lucy (1977), is a traditional mesh-free method. The MPS (Moving Particle Semi-implicit) is another typical particle-based mesh-free method, proposed by Koshizuka and Oka (1996). These mesh-free methods demonstrate many advantages while addressing the problems of intense free-surface flows because the boundaries of material can be tracked by particles automatically. Since the mesh-free methods are naturally effective to solve wave-plate interaction, researchers have done a large quantity of work. Tanaka and Masunaga (2010) studied the stabilization and smoothing of pressure in MPS method by quasi-compressibility. Lee et al. (2011) improved the MPS method in simulating violent free-surface motions and impact-loads. Khayyer and Gotoh (2009, 2010, 2011, 2016) proposed modified moving particle semi-implicit methods and then adopted a multiphase compressible–incompressible particle method to analyze the water slamming. Liu and Li (2016) adopted SPH (smoothed particle hydrodynamics) to analyze the modeling of viscous incompressible flows. Rao and Wan (2018) studied the wave-induced slamming force on the elastic plate. Gotoh and Khayyer (2016, 2018) concluded current achievements and further developments of the particle method. Sun et al. (2019a, 2019b) adopted the mixed mode function-modified MPS method to investigate the wave-structure dynamic interaction when the wave impacted on the cross deck of trimaran; he also applied modified MPS and modal superposition methods to the time-domain hydro elasticity computation of cylindrical shell and non-uniform beam structures.

Many investigationes regarding the submerged plate interacting with waves have been conducted. Li et al. (2010) carried out numerical simulation of the wave interacting with a submerged horizontal twin-plate and analyzed evolution of the wave and pressure acting on the plate. Zhang et al. (2013) analyzed the flow field around a submerged horizontal plate. Lo and Liu (2014) researched the solitary wave interacting with a submerged horizontal plate and discussed the wave pressure on the plate. Hayatdavoodi et al. (Hayatdavoodi and Ertekin, 2015a, 2015b; Hayatdavoodi et al., 2017) proposed a nonlinear model via the Level I Green-Naghdi theory to analyze the evolution of the fluid field and wave loads on a plate when the plate submerged in the water. Liu et al. (Liu and Li, 2016; Liu et al., 2009, 2017) implemented numerical simulation and experiments to investigate nonlinear scattering of non-breaking waves by a submerged horizontal plate; he also simulated a submerged horizontal plate heaving in regular waves and its performance as a breakwater was examined. He et al. (2018) applied SPH method to simulate the wave scattering by a heaving submerged horizontal plate. Wang et al. (2019) conducted numerical simulation regarding interaction between the water wave and a floating plate breakwater. These studies focus on the plate's influence on the wave evolution and wave pressure on the plate. Numerous factors including the wave height, submerged depth and thickness of the plate and moving or fixed plate will affect the result and we can find interesting phenomena after further investigation.

Owing to the advantage of mesh-free method, this paper implements MPS method to carry out a numerical simulation of the incompressible fluid flowing over a submerged, horizontal, thin, and rigid plate and numerical results are compared with those of the experiment performed at the State Key Laboratory of Coastal and Offshore Engineering, Dalian University of Technology, to verify the accuracy of the solver. The solitary waves are generated by a piston-type wave maker. Then the wave height, submerged depth and length of the plate are analyzed to study the influence of these three factors on the wave-structure interaction.

2 Numerical methods

In this paper, the MPS method is adopted in order to investigate the wave-plate interaction problem. The horizontal plate is rigid and fixed. The theory of the MPS and our in-house meshless particle CFD solver MLParticle-SJTU based on MPS method have been presented with details in our previous papers (Zhang and Wan, 2017; Zhang et al., 2012, 2014, 2016; Tang and Wan, 2015; Tang et al., 2016). Thus, brief description of them will be shown in this section.

2.1 Governing equations

The governing equations of the MPS method for viscous incompressible fluid can be expressed in Lagrangian form as follows:

$$\nabla \cdot \boldsymbol{V} = 0; \tag{1}$$

$$\frac{\mathrm{D}\boldsymbol{V}}{\mathrm{D}t} = -\frac{1}{\rho}\nabla P + v\nabla^2 \boldsymbol{V} + \boldsymbol{g}, \tag{2}$$

where $\boldsymbol{V}$, t, ρ, P, v and $\boldsymbol{g}$ represent the velocity vector, time, water density, pressure, kinematic viscosity and the gravity acceleration vector, respectively.

2.2 Kernel function

In MPS method, the particle interactions are based on the kernel function. In the present paper, a modified kernel function proposed by Zhang and Wan (2012) is adopted. The kernel function in the present paper can be formulated as:

$$W(r) = \begin{cases} \dfrac{r_\mathrm{e}}{0.85r + 0.15r_\mathrm{e}} - 1 & 0 \leqslant r < r_\mathrm{e} \\ 0 & r_\mathrm{e} \leqslant r \end{cases} \tag{3}$$

where $r = \left| r_j - r_i \right|$ is the distance between particle i and j, and r_e denotes the influence radius of the target particle. The advantage of this improved kernel function is that it can avoid the singularity at $r = 0$.

2.3 Discrete expressions of particle interaction models

In MPS, models of particle interaction involve the gradient, divergence, and Laplacian models. They are written as Eqs. (4)–(6):

$$\langle\nabla\phi\rangle_i=\frac{n_{\dim}}{n^0}\sum_{j\neq i}\frac{\phi_j+\phi_i}{|\boldsymbol{r}_j-\boldsymbol{r}_i|^2}(\boldsymbol{r}_j-\boldsymbol{r}_i)\cdot W\left(|\boldsymbol{r}_j-\boldsymbol{r}_i|\right); \tag{4}$$

$$\langle\nabla\cdot\boldsymbol{\Phi}\rangle_i=\frac{n_{\dim}}{n^0}\sum_{j\neq i}\frac{\left(\boldsymbol{\Phi}_j-\boldsymbol{\Phi}_i\right)\cdot\left(\boldsymbol{r}_j-\boldsymbol{r}_i\right)}{|\boldsymbol{r}_j-\boldsymbol{r}_i|^2}W\left(|\boldsymbol{r}_j-\boldsymbol{r}_i|\right); \tag{5}$$

$$\left\langle\nabla^2\phi\right\rangle_i=\frac{2n_{\dim}}{n^0\lambda}\sum_{j\neq i}(\phi_j-\phi_i)\cdot W\left(|\boldsymbol{r}_j-\boldsymbol{r}_i|\right), \tag{6}$$

where ϕ is an arbitrary scalar function, $\boldsymbol{\Phi}$ is an arbitrary vector, $n_{\dim}$ is the number of space dimensions, n^0 is the initial particle number density for incompressible flow, and λ is a parameter defined as:

$$\lambda=\frac{\sum_{j\neq i}W\left(|\boldsymbol{r}_j-\boldsymbol{r}_i|\right)\cdot|\boldsymbol{r}_j-\boldsymbol{r}_i|^2}{\sum_{j\neq i}W\left(|\boldsymbol{r}_j-\boldsymbol{r}_i|\right)}, \tag{7}$$

which is introduced to keep the variance increase equal to that of the analytical solution $\lambda=\int_V W(\boldsymbol{r})\cdot\boldsymbol{r}^2\mathrm{d}V\Big/\int_V W(\boldsymbol{r})\mathrm{d}V$ (Koshizuka et al., 1998).

2.4 Model of incompressibility

The incompressible condition of MPS method is represented by keeping the particle number density constant. In each time step, there are two stages: first, temporal velocity of particles is calculated based on viscous and gravitational forces, and particles are moved according to the temporal velocity; second, pressure is implicitly calculated by solving a Poisson Equation, and the velocity and position of particles are updated according to the obtained pressure. In the present paper, the mixed source term method combined with a velocity divergence-free condition and a constant particle number density (Tanaka and Masunaga, 2010; Lee et al., 2011) is employed and shown as follows:

$$\left\langle\nabla^2P^{n+1}\right\rangle_i=(1-\gamma)\frac{\rho}{\Delta t}\nabla\cdot\boldsymbol{V}_i^*-\gamma\frac{\rho}{\Delta t^2}\frac{\langle n^*\rangle_i-n^0}{n^0}, \tag{8}$$

where Δt denotes the calculation time step, n and n+1 indicate the physical quantity in the n-th and (n+1)-th time steps, and γ is the weight of the particle number density term between 0 and 1. In this paper, γ=0.01 is selected for all numerical experiments.

2.5 Detection of surface particles

In the MPS method, the free surface boundary conditions, including kinematic and dynamic boundary conditions, are required. In general, the dynamic condition is imposed by setting zero pressure on the free surface particles. Thus, the accurate detection of surface particle is paramount to the obtained pressure field. In the present paper, an improved surface particle detection method is implemented. This method is based on the asymmetry property. A vector function $\boldsymbol{F}$ is introduced as follows to represent the asymmetry of arrangements of neighbor particles.

$$\langle\boldsymbol{F}\rangle_i=\frac{n_{\dim}}{n^0}\sum_{j\neq i}\frac{1}{|\boldsymbol{r}_i-\boldsymbol{r}_j|}(\boldsymbol{r}_i-\boldsymbol{r}_j)W(\boldsymbol{r}_{ij}), \tag{9}$$

where the vector function $\boldsymbol{F}$ represents the asymmetry of arrangements of neighbor particles. Particle satisfying:

$$\langle|\boldsymbol{F}|\rangle_i>0.9|\boldsymbol{F}|^0 \tag{10}$$

is considered as a free surface particle, where $|\boldsymbol{F}|^0$ is the initial value of $|\boldsymbol{F}|$ for the surface particle.

2.6 Solving procedure of MPS

The projection-correction algorithm is employed in the solving process of MPS method. The procedure is demonstrated step by step as follows.

(1) Predict the temporal particle velocity and position explicitly under mass and viscous force.

$$\boldsymbol{V}^*=\boldsymbol{V}^n+\Delta t\cdot\left(\nu\nabla^2\boldsymbol{V}+\boldsymbol{g}\right); \tag{11}$$

$$r^*=r^n+\Delta t\cdot\boldsymbol{V}^*. \tag{12}$$

(2) Calculate the particle number density n* of the temporal state.

(3) Solve the pressure Poisson equation and obtain the particle pressure at the next time step.

(4) Correct the velocity and position of particles implicitly based on the obtained pressure.

$$\boldsymbol{V}^{n+1}=\boldsymbol{V}^*-\frac{\Delta t}{\rho}\cdot\nabla p^{n+1}; \tag{13}$$

$$r^{n+1}=r^n+\Delta t\cdot\boldsymbol{V}^*. \tag{14}$$

2.7 Generation of numerical wave

According to the potential flow theory, a solitary wave consists of a single crest of infinite length. The profile of the solitary wave can be expressed as follows (Korteweg and de Vries, 1895):

$$\eta=A\mathrm{sech}^2\left[k(x-ct)\right]; \tag{15}$$

$$k=\sqrt{3A/(4H^3)}; \tag{16}$$

$$c=\sqrt{g(A+H)}, \tag{17}$$

where A is the wave amplitude for solitary wave. H, x and c denote the water depth, the horizontal coordinate and the wave speed, respectively. In this paper, the solitary wave is generated by a piston-type wave maker, whose motion was described by Goring (1978). The speed of the wave maker is formulated as:

$$U(t)=\frac{\mathrm{d}X(t)}{\mathrm{d}t}=\frac{cA\mathrm{sech}^2\left[k(X-ct)\right]}{d+A\mathrm{sech}^2\left[k(X-ct)\right]}, \tag{18}$$

where X and d denote the position of the wave maker and water depth, respectively. Thus, the position of the wave maker at time t can be expressed as:

$$X(t) = \frac{A}{kd}\tanh[k(ct - X)]. \tag{19}$$

The stroke length is calculated by the difference value between the wave maker position at $t = +\infty$ and $t = -\infty$:

$$S = \sqrt{16AH/3}. \tag{20}$$

The wave period is approximately:

$$T \approx \frac{2}{kc}\left(3.8 + \frac{A}{H}\right). \tag{21}$$

After one wave period, the wave maker reaches its maximum position and then becomes still.

3 Numerical simulation

In this section, the interaction between the solitary wave and a horizontal plate is investigated based on the aforementioned MPS method. Fig. 1 shows the model of the numerical wave tank without a plate. Table 1 shows the computatonal parameters. The tank is 4.00 m in length and the water depth (h) is 0.3 m. As is shown, the left side piston is employed to generate the solitary wave.

3.1 Generation of the numerical wave

Before studying the wave–structure interaction, it is essential to examine the accuracy of the solitary wave generation. Thus, the verification is conducted in the numerical wave tank without the plate. The piston type wave maker is employed to generate the solitary wave. Different wave amplitudes (A), including A/h = 0.23, 0.33, 0.4 and 0.5, are adopted in the simulation. The numerical results are compared with the theoretical solution by solving Eq. (15).

Fig. 2 shows the comparison of the wave profile between the numerical simulation and the theoretical solution. We can see that the peak of wave height and the pattern of evolution agree well with those of the theoretical solution in different time. However, there are still some slight distinctions, such as the ascending portion of the curve, because of the finite length of the tank and depth of water. So, the method generating wave in this paper is accurate enough.

3.2 Interaction between the wave and a 2D plate

In this subsection, the interaction between a two-dimensional submerged, horizontal, fixed and rigid plate and the solitary wave is simulated with the help of the in-house MPSFEM-SJTU solver. The plate is located at the position of 1.0 m away from the wave maker. The distance between the top of the plate and the still water line (SWL) is defined as plate submerged depth (D), which can be altered by moving the plate vertically in next subsection to investigate the influence of the submerged depth on the interaction between the plate and the wave. The surface elevation and pressure on the upper and lower surfaces of the plate are recorded and compared with those of the experiment to verify the accuracy of the solver. The experiment is conducted at the State Key Laboratory of Coastal and Offshore Engineering, Dalian University of Technology. In the experiment, the tank is 20.00 m in length and the water depth (h) is 0.3 m. The plate is 0.25 m long and the submerge depth is 0.1 m. The distance between the leading end of the plate and the wave maker is 9.2 m. Time series of the surface elevations at six positions were recorded. The time interval of sampling points was set as 0.02 s. Pressure sensors with sampling rate of 400 Hz are used to measure the pressure induced by the solitary waves. In the numerical simulation, the length of the tank is shortened to 4 m. The model of the numerical wave tank with a plate and parameters of the case are shown in Fig. 3 and Table 2, respectively.

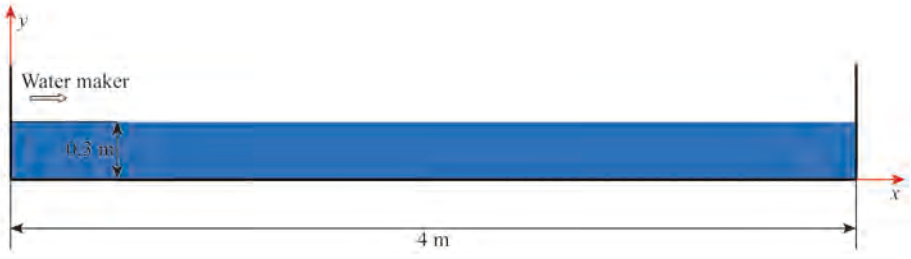

Fig. 1. Geometric model of the numerical wave tank.

Table 1 Computational parameters

Parameter	Value
Water density	1000 kg/m^3
Water depth	0.3 m
Kinematic viscosity	1×10^{-6} m^2/s
Gravitational acceleration	9.81 m/s^2
Particle spacing	0.0075 m
Fluid particle number	78618
Total particle number	78618

As illustrated in Fig. 4, the leading edge of the plate is chosen as the temporal time origin. The pressure is the hydrodynamic pressure which equals the difference between the total pressure and the hydrostatic pressure. Some snapshots of the simulation are presented in Fig. 5. It can be observed that the crest of the wave arrives at the leading edge of the plate at t=1.28 s. Then, the wave flows over the plate. The wave height decreases after the wave flowing over the

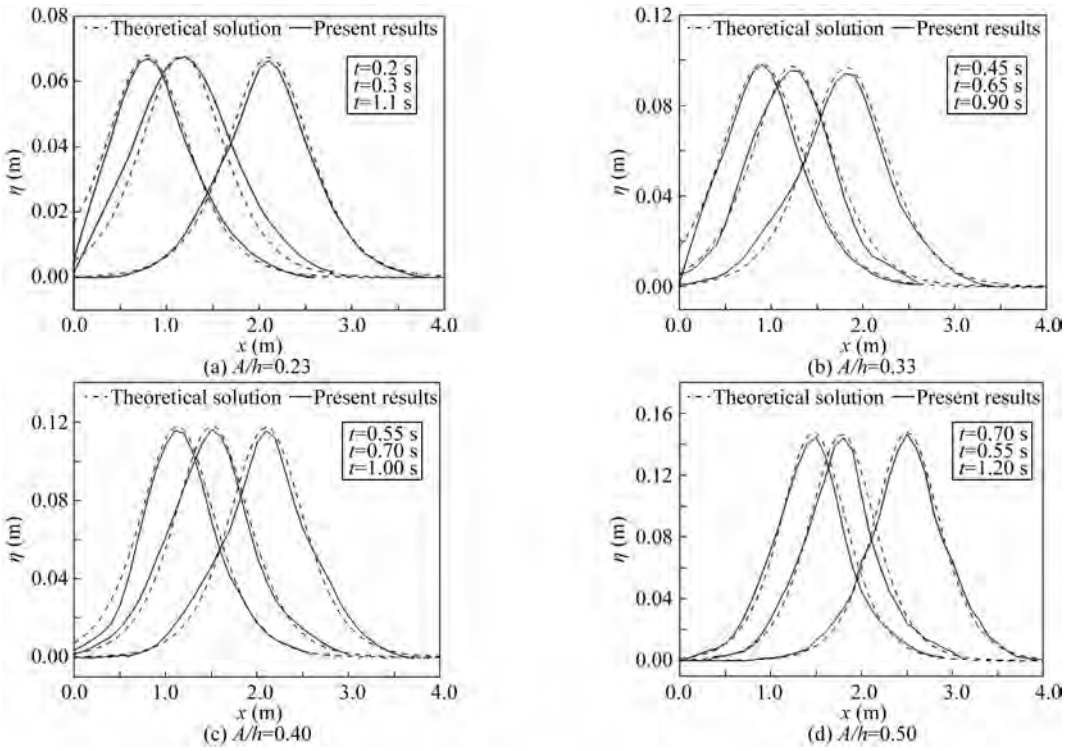

Fig. 2. Wave elevation of theoretical solution and present results.

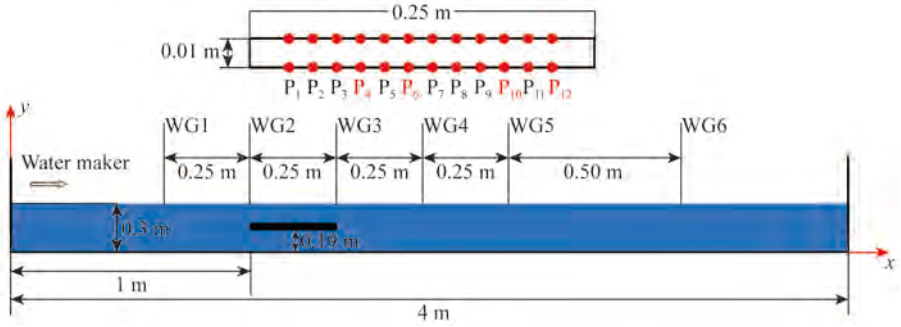

Fig. 3. Geometric model of the numerical wave tank.

Table 2 Parameters of the case

Water depth (cm)	Plate thickness (cm)	Submerged depth (cm)	Wave amplitude (cm)	*A*/*h*
30	1	10	7	0.23

plate.

The numerical simulation and experimental surface elevation of four points (WG1, WG2, WG3, WG4, shown in Fig. 3) in the tank are compared in Fig. 6. Numerical results have a close agreement with the experimental data. The maximum wave height is approximately equal to the given wave height and the wave pattern also has a similar tendency. The peak of history curves of wave height decreases along the flow direction due to the loss of wave energy during the flow. That is because the presence of the plate will disturb the flow and reflect part of energy, all of which will reduce the wave energy.

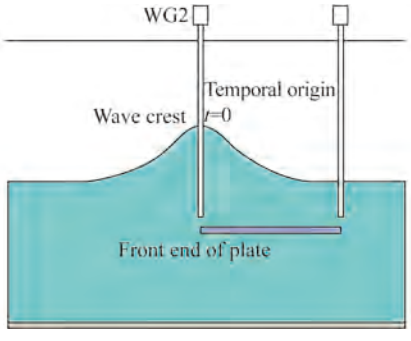

Fig. 4. Definition of temporal origin.

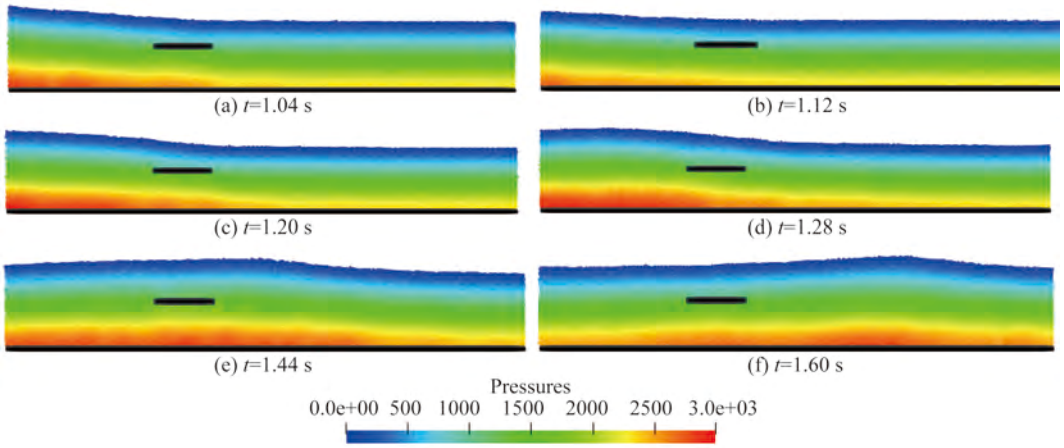

Fig. 5. Snapshots of pressure fields.

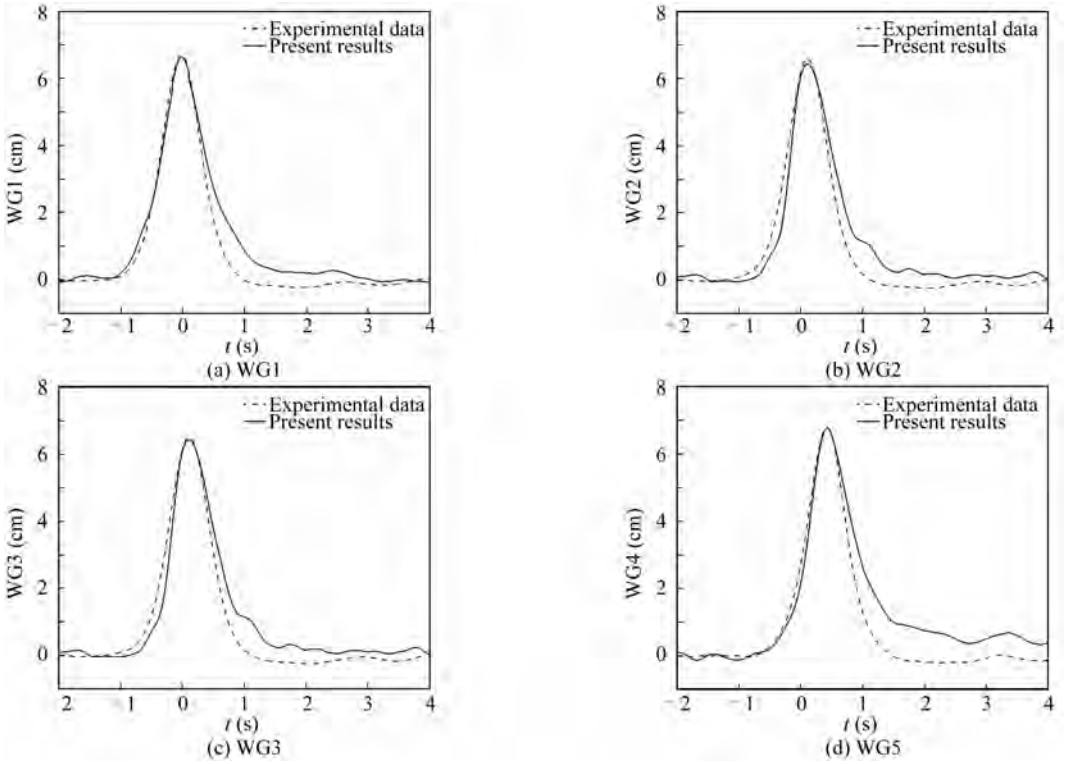

Fig. 6. Wave elevation on the wave gauge.

The hydrodynamic pressure of points arranged in the upper and lower surfaces of the plate is illustrated in Figs. 7a and 7b. We notice that the hydrodynamic pressure on the plate, which equals the difference between the total pressure and the hydrostatic pressure, is oscillating around the equilibrium position. The peak of pressure occurs at the place where the crest of the wave arrives simultaneously. The numerical results agree well with those of the experiment. The peak of history curves of pressure among different points is not always similar, because the presence of the plate influences the wave propagation.

In Fig. 8, the numerical maximum pressure on the upper and lower surfaces of the plate is compared with experimental results respectively. As for the plate's upper surface pressure, the pressures of both the numerical simulation and the experiment have the same tendency, and the pressure along the plate is not necessarily the same. Pressure of the plate reduces from P4 to P6, then increases from P6 to P10, finally from P10 to P12, and the pressure declines again. The changing tendency of pressure is caused by the presence of the plate. When the solitary wave approaches the plate, in the midpoint of the plate (P6), the water depth above the plate suddenly reduces and the wave height increases. Because the wave energy partly converts to poten-

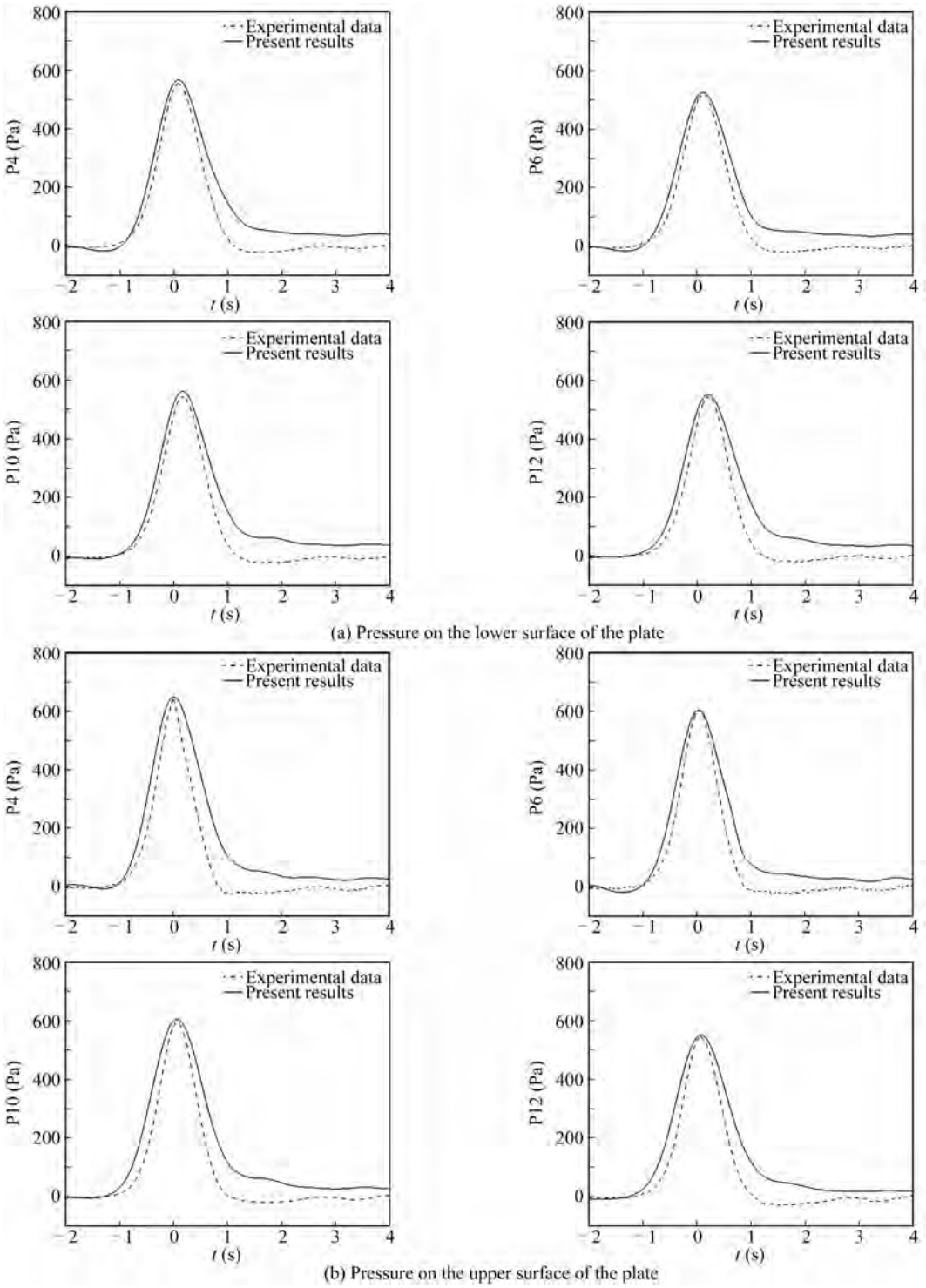

Fig. 7. History of pressure of the plate.

tial energy, the hydrodynamic pressure of P6 declines and is relatively small as compared with that of P4. When the wave flows away from the plate, the water depth recovers and the hydrodynamic pressure of P10 increases, so the pressure of P10 is larger than that of P6. As for the pressure of P12, due to energy loss caused by the presence of the plate, the pressure does not recover to the pressure level of P4. The pressure change on the upper surface and lower surface has the same tendency.

Moreover, the plate's bottom and top surface pressure is also not necessarily the same, which is shown in Figs. 8c and 8d. First, it is noticeable that the pressure of the upper surface is relatively larger than that of the lower surface, because the wave velocity drops along the vertical direction and the hydrodynamic pressure also reduces along the perpendicular direction. Therefore, the pressure of the upper

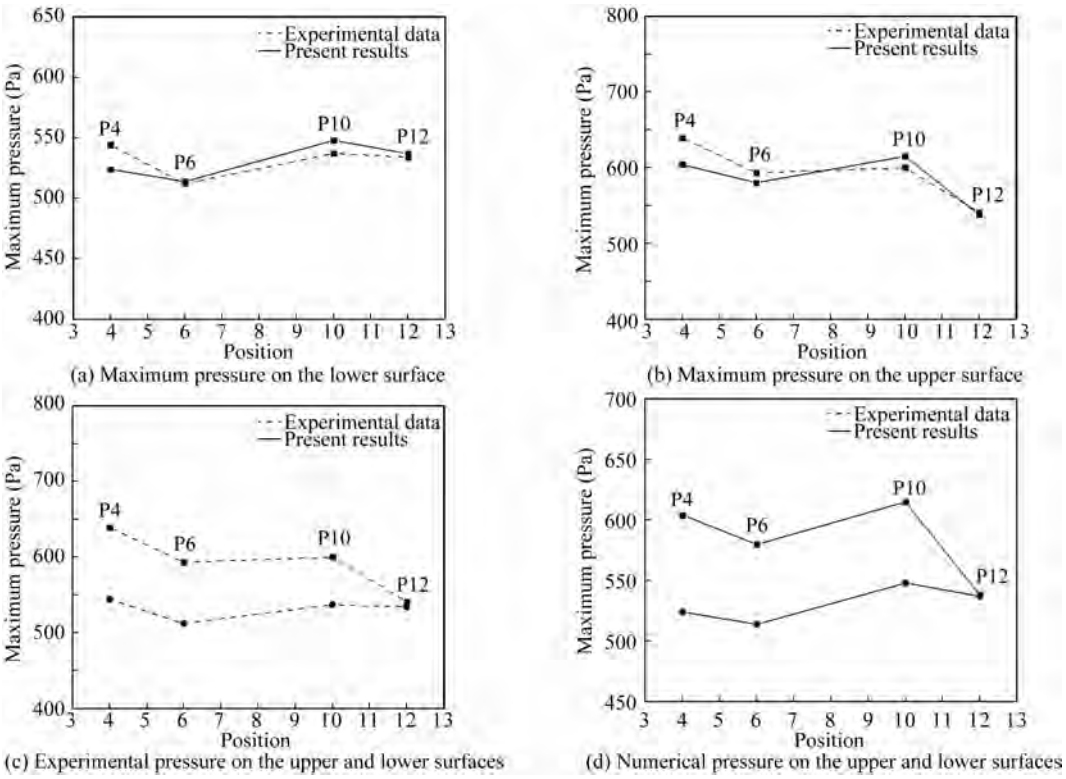

Fig. 8. Maximum pressure on the upper and lower surfaces of the plate.

surface is larger than that of the lower surface. Second, the difference between the upper and lower surface pressure is not necessarily the same. The thickness of the plate causes a theoretical difference of hydrodynamic pressure on the plate's upper and lower surfaces due to the different water depths. However, those pressure differences along the plate are not uniform. The difference at the leading edge of the plate (P4) is large, while at the tail edge (P12), the difference is small, because the plate influences the wave velocity. At the leading edge, the difference of wave velocity under and above the plate is large and the difference of hydrodynamic pressure is palpable. When the wave flows over the plate, the velocity differential under and above the plate drops and the differences of pressure also decrease. Thus, the fixed plate influences the pressure under and above the plate by influencing the wave propagation. In a word, the fixed plate will affect the velocity fields to influence the pressure distribution above and under the plate.

3.3 Influence of wave height

Many factors, including the wave height, submerged depth and length of the plate, affect the interaction between the plate and the wave and are worthwhile to be investigated. In this subsection, the influence of the wave height on the interaction between the plate and the solitary wave will be discussed. Four cases, when A/h equals 0.23, 0.33, 0.4 and 0.5, are adopted in the simulation. The parameters of cases are listed in Table 3.

In Fig. 9, the wave elevations on four gauges including WG1 (x=0.75 m), WG2 (x=1.0 m), WG3 (x=1.25 m) and WG4 (x=1.5 m) are shown. In order to compare the interaction between the solitary waves with different heights and a plate, the wave elevation curves of different gauges are moved to the same phase and the wave height and the time are dimensionless. The horizontal time axis corresponds to the record of WG1. Records of other gauges are shifted (in time) to match the wave of WG1. Thus, a comparison of the wave at different gauges can be made.

In Fig. 9, it can be seen that the solitary wave propagation speed increases, when wave records of WG1 from Fig. 9a to Fig. 9d are compared, because the wave peak passing through the wave gauge WG1 is increasing in shorter time due to the increase of the wave height. It can also be

Table 3 Numerical parameters for the submerged cases

Case	Water depth (cm)	Plate thickness (cm)	Submerged depth d (cm)	Wave height H (cm)	A/h
A	30	1	10	7	0.23
B	30	1	10	10	0.33
C	30	1	10	12	0.40
D	30	1	10	15	0.50

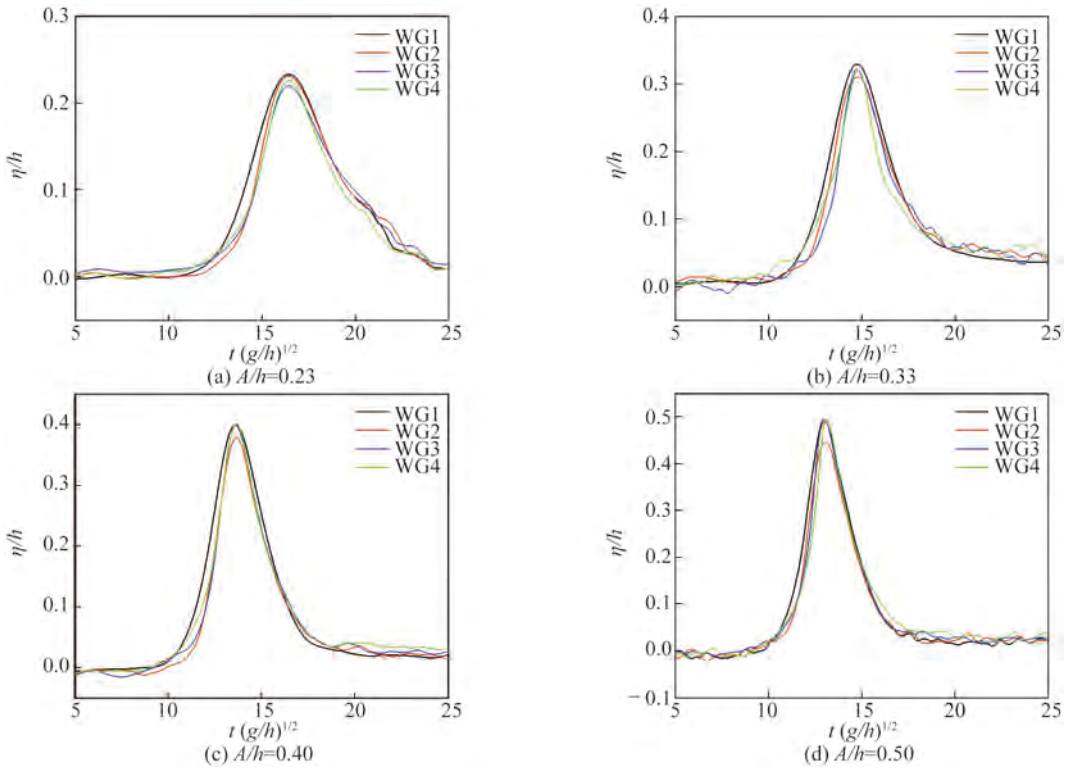

Fig. 9. Wave elevations on the wave gauge.

observed that the wave heights in different gauges are not necessarily the same. In all cases, the solitary wave amplitude above the plate (WG2) is dropped slightly compared with the wave height in WG1 due to the energy attenuation. However, after the initial drop, when the wave transmits over the plate (WG3, WG4), the solitary wave amplitude (WG3, WG4) increases owing to smaller water depth. As the wave amplitude increases as shown in Fig. 10, the effect of the plate on wave propagation is ever more obvious. Hence, the presence of the plate does influence the wave propagation. When the wave height increases, this impact will become more palpable.

Fig. 10 shows the maximum pressure acting on the upper and lower surfaces of the plate. In Figs. 10a and 10b, both the upper and lower surface pressure increases with the increase of the wave height. That is because the wave velocity increases and the wave hydrodynamic pressure is proportional to the velocity. It is also interesting to see that the pressure among different gauges is not necessarily the same. In all cases, on the upper surface of the plate in Fig. 10a, the maximum pressure in the middle of the plate (P6) is small when compared with the pressure at the edge of the plate (P4, P10 and P12). That is because the water depth suddenly decreases above the plate due to the presence of the plate. The wave propagates from the deep water to shallow water and the wave height initially decreases and then increases. Thus, the wave velocity and hydrodynamic pressure decrease. After the wave flows over the plate, the wave

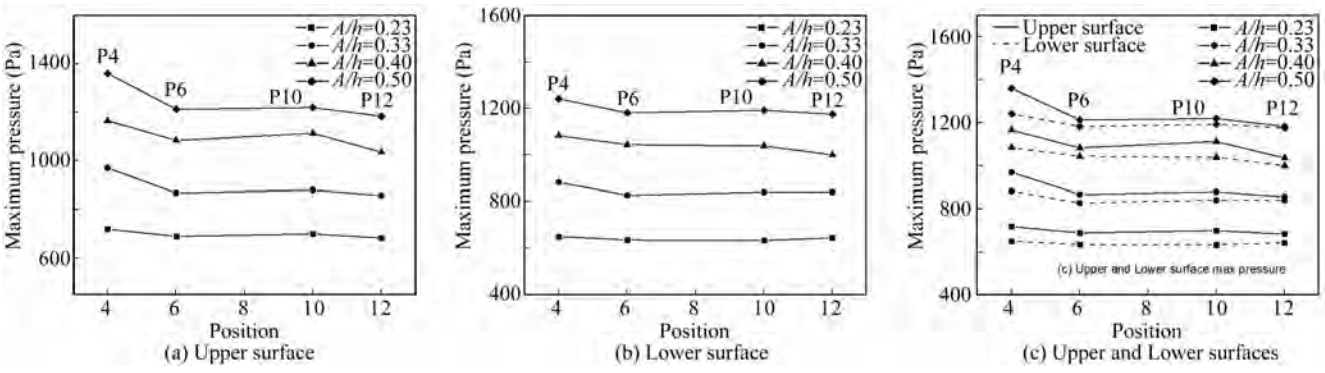

Fig. 10. Maximum pressure on the upper and lower surfaces of the plate.

propagates from the shallow water to deep water and the pressure increases relatively. However, on the lower surface of the plate in Fig. 10b, the pressure along the down wave direction linearly declines and the energy loss resulted from the presence of the plate is the key factor.

On the upper surface of the plate, as the wave height increases, the influence of the plate on the wave propagation becomes more obvious. In Case D (A/h=0.5), the wave height is the largest and the influence of the plate is the most significant. The reduction of the pressure from P4 to P6 is the most obvious. It corresponds to the most remarkable wave elevation change in Fig. 9, because the increasing wave height makes the influence of the plate on the wave propagation above the plate more noticeable. As for the lower surface of the plate, the influence of the wave height is not noticeable. When the wave height increases, in all cases, the pressure change along the flow direction is almost linear and has a similar tendency. Thus, the impact of the wave height on the pressure change of the lower surface along the flow direction is not obvious. Fig. 10c also indicates the pressure differences between the upper and lower surfaces. In all cases, the pressure difference reduces from P4 to P12 and the pressure difference of P4 is the biggest compared with that of other gauges. With the wave height increasing, the large wave height can expand pressure differences in P4.

Finally, we can draw a conclusion that the wave height actually has influences on the wave propagation above the plate. That is because the plate causes the sudden reduction of the water depth and this effect becomes greater, when the wave height increases. Hence, a submerged plate can act as an effective tool for protecting marine structures or coastlines from the wave damage. In next subsection, this paper will further investigate the influence of the plate submerged depth.

3.4 Influence of the plate position

In this subsection, the immersion plate's position is analyzed. The water depth h is 0.3 m and the submerged depth is set as d/h=0.13, 0.23, 0.33 and 0.5 to investigate the influence of the plate position. The wave height is 0.1 m in four cases.

In Fig. 11, time series of wave elevation when the plate is placed at different depths are shown. As shown in Fig. 11a, when the plate is closest to the SWL, d/h = 0.13, it has the most significant impact on the wave propagation. In this case, the wave above the plate (WG2) undergoes obvious deformation when compared with the wave recorded in WG1. The wave above the plate (WG2) has small amplitude, although the wave amplitude increases when the wave propagates over the plate (WG3, WG4). The increase of the wave height after the initial drop is caused by the smaller water depth. As the submerged depth increases, the deformation of the wave and the decrease of the wave height decline. It indicates that the influence of the plate decreases with the increase of the plate submerged depth.

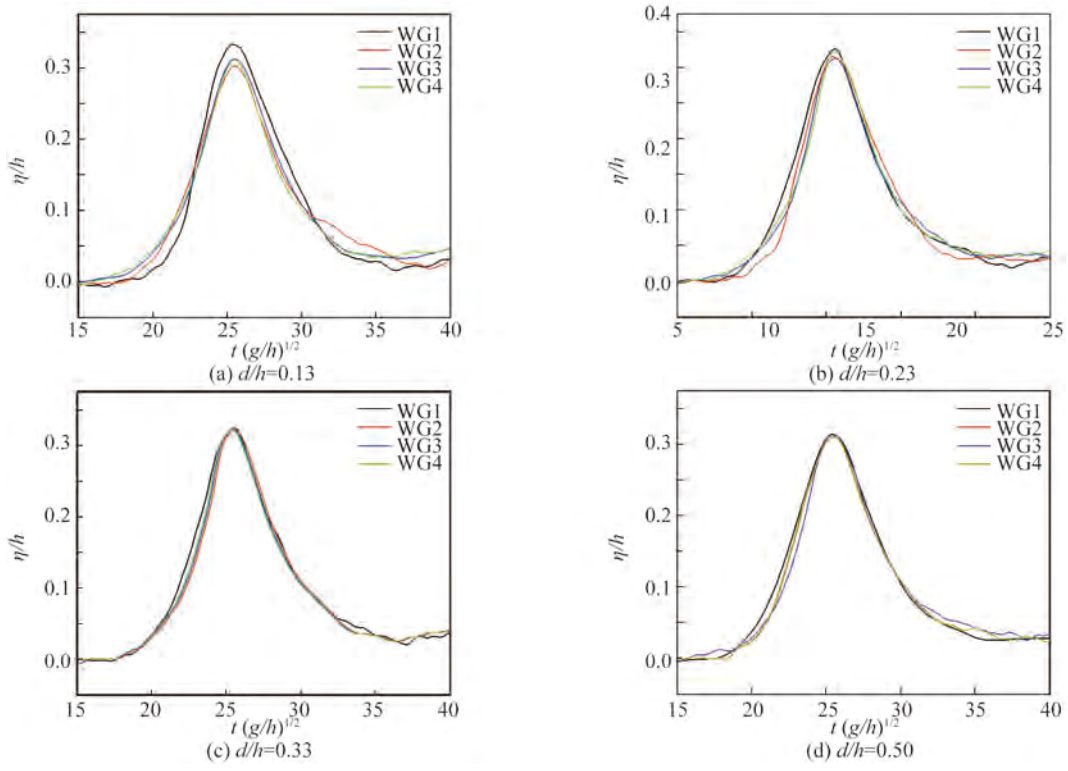

Fig. 11. Wave elevation on the wave gauge.

When the depth is large enough, the influence can be ignored. In all cases, the down wave has recovered its original form. To conclude, when the plate is close to SWL, the wave undergoes the deformation and the reduction of wave height and recovers its original form after flowing over the plate. As the submerged depth arrives at a critical point, the plate's influence can be ignored.

In Fig. 12, the maximum pressure on the upper and lower surfaces of the plate is shown. Both the upper and lower surface pressures decrease with the increase of the submerged depth. That is because the hydrodynamic pressure is inversely proportional to the water depth. It is also interesting to see that the pressure among different gauges is not necessarily the same. On the upper surface of the plate, in all cases, the presence of the plate influences the pressure. When the submerged depth is d/h=0.13, where the plate is closest to the SWL, from P4 to P6, the pressure on the plate decreases first and then increases from P6 to P10 and P12. That is because the water above the plate suddenly becomes shallow and the water depth recovers behind the plate. On the lower surface of the plate, the pressure drops linearly along the wave flow direction.

On the upper surface, as the submerged depth increases, the plate's influence on the wave becomes less significant, which is shown in Fig. 12a. When the depth is equal to d/h=0.33, the upper surface pressure changes almost linearly from P4 to P12. That is because the plate's submerged depth is large enough and the water above the plate is deep enough and has less effect on the wave propagation. In Fig. 12b, as for the lower surface of the plate, the increasing depth has less effect on the pressure and the pressure declines linearly in all cases. As for the pressure difference between the upper and lower surface, different gauges have different pressure differences, as shown in Fig. 12c. When the submerged depth is d/h=0.13, the pressure in P4 above the plate drops due to shallow water and the pressure difference between upper and lower surfaces in P4 is small when compared with that of other pressure gauges in this case. However, in other cases, when the submerged depth increases, pressure differences between the upper and lower surfaces in all gauges do not have an obvious discrepancy, because the plate has less effect on wave propagating over the plate.

In a word, the plate's immersion depth has significant impact on the wave propagation and a critical submerged depth in which the plate's influence can be ignored exists for a certain wave. Therefore, a certain structure can be designed to attenuate the wave's impact for the practical application, like protecting the beach from erosion. Since the plate submerged depth is an important factor in the wave and plate interaction, in the next subsection, the paper will further study the influence of another factor, the plate length.

3.5 Influence of the plate length

In this subsection, the plate length is discussed. The water depth h is 0.3 m. In order to study the influence of plate's length on the interaction between the solitary wave and the plate, the plate's length is set as l/h=0.8, 1.5, 2.2 and 2.8. The wave height is 0.1 m in four cases.

In Fig. 13, the wave elevation, when the plate's length is different, is presented. The most significant impact of the plate length on the solitary wave is perceived at WG2, above the plate. The wave height initially drops in WG2 due to the presence of the plate and then increases in WG3 when the wave transmits to the shallow water above the plate. As the plate length increases, the initial wave amplitude reduction relatively increases. However, in all cases, the wave finally recovers its form. That is because in cases of different plate lengths, the water depth above the plate is constant. Therefore, the wave propagation seems to be independent of the plate length and the plate length has little effect on the scattering of the solitary wave.

Fig. 14 shows the maximum pressures on the upper and lower surfaces of the plate. The difference between the upper and lower surface pressures exists. Above the plate, when the wave flows through the plate, the pressure acting on the plate decreases from P4 to P6 due to the sudden decrease of the water depth. Then from P6 to P10 and P12, the pressure recovers but does not arrive at the initial value due to the energy attenuation. The procedure is nonlinear.

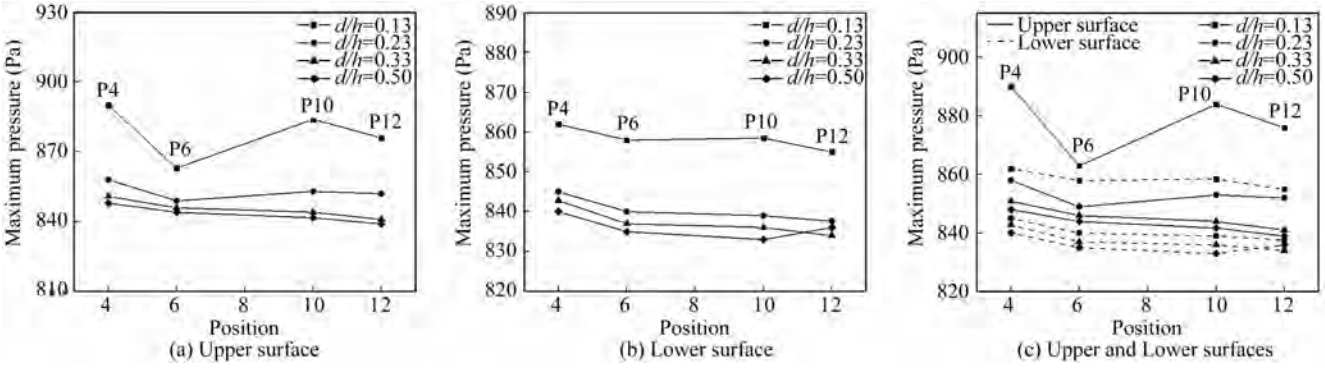

Fig. 12. Maximum pressure on the upper and lower surfaces of the plate.

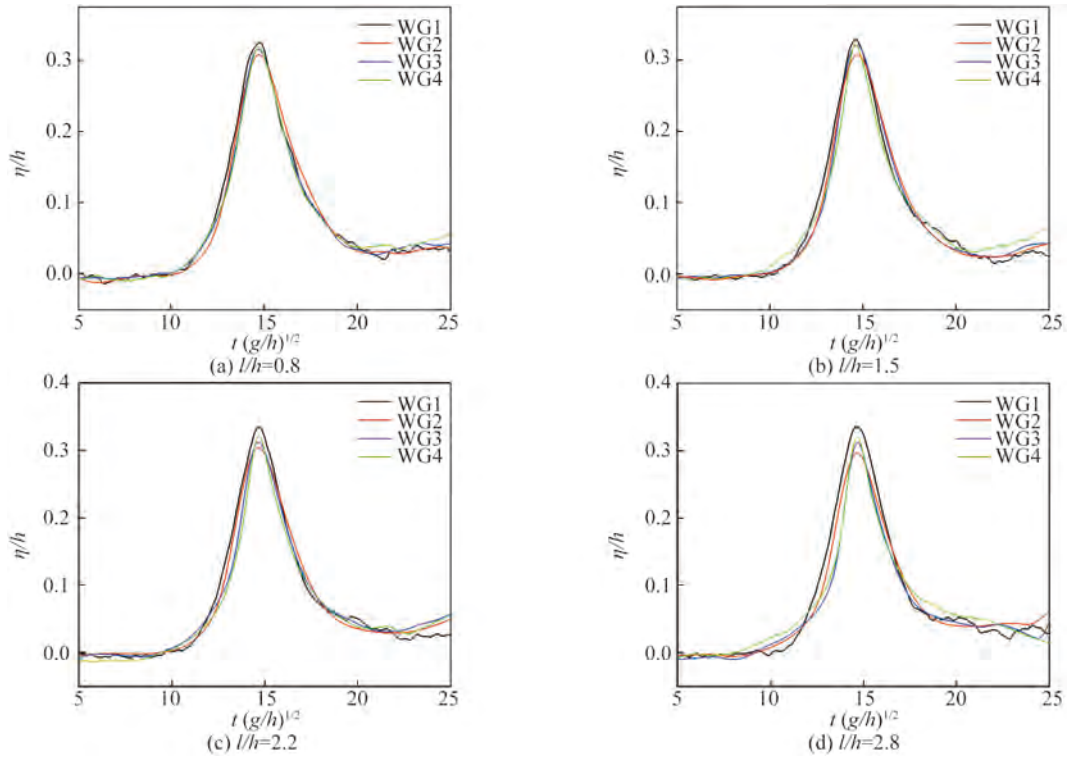

Fig. 13. Wave elevation on the wave gauge.

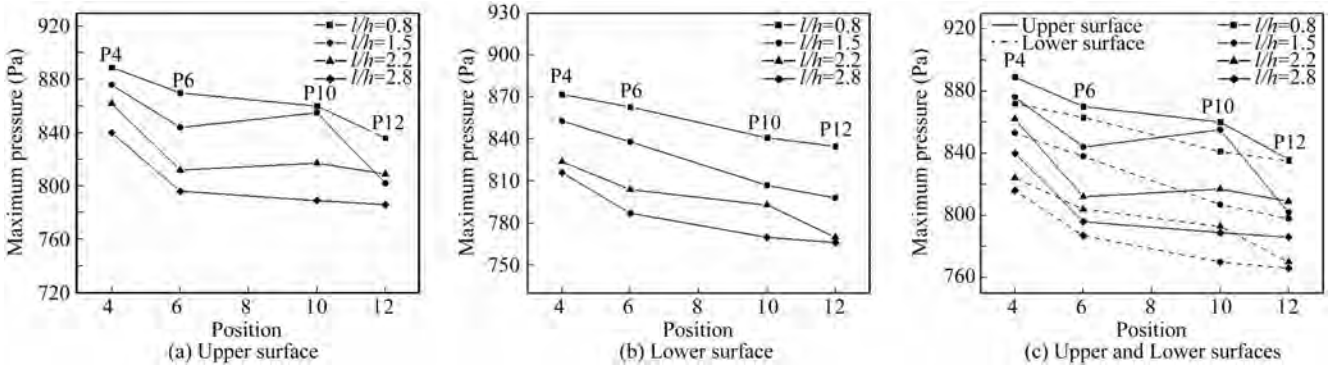

Fig. 14. Maximum pressure on the upper and lower surfaces of the plate.

However, on the lower surface, the pressure drops linearly and has no obvious turning point. That is because the plate has less effect on the wave under the plate. As the length of the plate increases, on the upper surface of the plate, in four cases, the pressure decreases and then increases due to the shallow water and the procedure in four cases has the same tendency; on the lower surface, the difference between four cases is not significant. As for the upper and lower surface pressure difference, in all cases, there is no obvious difference of the pressure distribution along the plate. That is because the plate's length has influences on the solitary wave above the plate but the length of the plate has less effect on wave transmitting through it. The increasing plate length just increases the area which the wave passes through. When the wave flows over the plate, the wave amplitude and wave form recovers to a great extent. However, the conclusion regarding the plate length's influences in this subsection can only be applied to the solitary wave. That is because the solitary wave length is infinite. The plate length is finite and has less effect. As for other kinds of waves, such as cnoidal wave (Hayatdavoodi et al., 2017), different conclusions can be drawn, because the wave length and plate length are the same order of magnitude and the plate length will be an important factor. Thus further investigation regarding different types of waves can be carried out and many interesting phenomena can be found.

4 Conclusions

In the present paper, the numerical simulation regarding the interaction between solitary wave and a two-dimension-

al submerged, fixed, horizontal rigid plate is carried out. First, four wave amplitudes (A), including A/h = 0.23, 0.33, 0.4 and 0.5, are adopted in the simulation. The numerical results are compared with the theoretical solution to verify the wave generation. Then, numerical results are compared with the laboratory experimental data, which is carried out at the State Key Laboratory of Coastal and Offshore Engineering, Dalian University of Technology, and the close agreement verifies the accuracy and application of our in-house MPSFEM-SJTU solver. The pressure in different positions of the plate is not necessarily the same. It is easy to observe that the plate affects the distribution of the pressure along the plate. The wave height above the plate initially drops and then increases when the water suddenly becomes shallow. It corresponds to the changes of pressure on the plate. In order to further investigate the factors, including the wave height, the plate submerged depth and the plate length, which influence the interaction between the solitary wave and a submerged plate. This paper designs four cases for each factor to study the plate's influence. As for the wave height, when the wave height increases, A/h= 0.23−0.50, the plate's effect on the wave propagation above the plate increases. As for the plate submerged depth, when the submerged depth increases, d/h=0.13−0.50, the plate's effect on the wave above the plate attenuates. When the submerged depth exceeds a certain critical depth, the plate's effect can be ignored. So, it has a practical application to design a structure to eliminate the wave energy to prevent the wave from damaging the structure like protecting benches from the wave erosion. As for the third factor, the plate length, in four cases with different plate lengths, l/h=0.8−2.8, remarkable differences regarding the plate's effect do not exist. So, the plate length has less effect on the wave transmitting through the plate.

In a word, as for the wave height, it has influences on the wave evolution and impacting pressure on the upper and lower surfaces. When the wave amplitude increases, the effect of the plate on the wave becomes more obvious. The submerged depth of the plate has a prominent influence on the wave evolution, when the submerged depth exceeds a certain critical depth, the plate's effect can be ignored. The length of the plate has less influence on the wave evolution. Further researches should be carried out to analyze the influence of different factors including different waves, and 3D effects on the interaction between the wave and the plate. Since the flexibility of the plate will influence the interaction between the wave and the plate (Khayyer et al., 2018a, 2018b), we should also consider cases when hydroelasticity effects are taken into account.

References

Anastasiou, K. and Shih, R.W.K., 1992. A laboratory study of the wave-induced vertical loading on platform decks, *Proceedings of the ICE-Water Maritime and Energy*, 96(1), 19–33.

Goring, D.G., 1978. *Tsunamis-the Propagation of Long Waves onto A Shelf*, Ph.D. Thesis, California Institute of Technology, Pasadena, California, USA.

Gotoh, H. and Khayyer, A., 2016. Current achievements and future perspectives for projection-based particle methods with applications in ocean engineering, *Journal of Ocean Engineering and Marine Energy*, 2(3), 251–278.

Gotoh, H. and Khayyer, A., 2018. On the state-of-the-art of particle methods for coastal and ocean engineering, *Coastal Engineering Journal*, 60(1), 79–103.

Greco, M., Colicchio, G. and Faltinsen, O.M., 2009. Bottom slamming for a very large floating structure: Coupled global and slamming analyses, *Journal of Fluids and Structures*, 25(2), 420–430.

Hayatdavoodi, M. and Ertekin, R.C., 2015a. Wave forces on a submerged horizontal plate-Part I: Theory and modelling, *Journal of Fluids and Structures*, 54, 566–579.

Hayatdavoodi, M. and Ertekin, R.C., 2015b. Wave forces on a submerged horizontal plate-Part II: Solitary and cnoidal waves, *Journal of Fluids and Structures*, 54, 580–596.

Hayatdavoodi, M., Ertekin, R.C. and Valentine, B.D., 2017. Solitary and cnoidal wave scattering by a submerged horizontal plate in shallow water, *AIP Advances*, 7(6), 065212.

Hayatdavoodi, M., Seiffert, B. and Ertekin, R.C., 2014. Experiments and computations of solitary-wave forces on a coastal-bridge deck. Part II: Deck with girders, *Coastal Engineering*, 88, 210–228.

He, M., Xu, W.H., Gao, X.F. and Ren, B., 2018. SPH simulation of wave scattering by a heaving submerged horizontal plate, *International Journal of Ocean and Coastal Engineering*, 1(2), 1840004.

Irajpanah, K., 1983. *Wave Uplift Force on Horizontal Platform*, Ph.D. Thesis, University of Southern California, Los Angeles, USA.

Khayyer, A. and Gotoh, H., 2009. Modified moving particle semi-implicit methods for the prediction of 2D wave impact pressure, *Coastal Engineering*, 56(4), 419–440.

Khayyer, A. and Gotoh, H., 2010. A higher order Laplacian model for enhancement and stabilization of pressure calculation by the MPS method, *Applied Ocean Research*, 32(1), 124–131.

Khayyer, A. and Gotoh, H., 2011. Enhancement of stability and accuracy of the moving particle semi-implicit method, *Journal of Computational Physics*, 230(8), 3093–3118.

Khayyer, A. and Gotoh, H., 2016. A multiphase compressible-incompressible particle method for water slamming, *International Journal of Offshore and Polar Engineering*, 26(1), 20–25.

Khayyer, A., Gotoh, H., Falahaty, H. and Shimizu, Y., 2018a. An enhanced ISPH-SPH coupled method for simulation of incompressible fluid-elastic structure interactions, *Computer Physics Communications*, 232, 139–164.

Khayyer, A., Gotoh, H., Falahaty, H. and Shimizu, Y., 2018b. Towards development of enhanced fully-Lagrangian mesh-free computational methods for fluid-structure interaction, *Journal of Hydrodynamics*, 30(1), 49–61.

Korteweg, D.J. and De Vries, G., 1895. On the change of form of long waves advancing in a rectangular canal and on a new type of long stationary waves, *The London*, *Edinburgh*, *and Dublin Philosophical Magazine and Journal of Science*, 39(240), 422–443.

Koshizuka, S., Nobe, A. and Oka, Y., 1998. Numerical analysis of breaking waves using the Moving Particle Semi-implicit method, *International Journal for Numerical Methods in Fluids*, 26(7), 751–769.

Koshizuka, S. and Oka, Y., 1996. Moving-particle semi-implicit method for fragmentation of incompressible fluid, *Nuclear Science and*

Engineering, 123(3), 421–434.

Lee, B.H., Park, J.C., Kim, M.H. and Hwang, S.C., 2011. Step-by-step improvement of MPS method in simulating violent free-surface motions and impact-loads, *Computer Methods in Applied Mechanics and Engineering*, 200(9−12), 1113–1125.

Li, J.B., Zhang, N.C. and Guo, C.S., 2010. Numerical simulation of waves interaction with a submerged horizontal twin-plate breakwater, *China Ocean Engineering*, 24(4), 627–640.

Liu, C.R., Huang, Z.H. and Chen, W.P., 2017. A numerical study of a submerged horizontal heaving plate as a breakwater, *Journal of Coastal Research*, 33(4), 917–930.

Liu, C.R., Huang, Z.H. and Tan, S.K., 2009. Nonlinear scattering of non-breaking waves by a submerged horizontal plate: Experiments and simulations, *Ocean Engineering*, 36(17−18), 1332–1345.

Liu, M.B. and Li, S.M., 2016. On the modeling of viscous incompressible flows with smoothed particle hydro-dynamics, *Journal of Hydrodynamics*, 28(5), 731–745.

Lo, H.Y. and Liu, P.L.F., 2014. Solitary waves incident on a submerged horizontal plate, *Journal of Waterway, Port, Coastal, and Ocean Engineering*, 140(3), 04014009.

Lucy, L.B., 1977. A numerical approach to the testing of the fission hypothesis, *The Astronomical Journal*, 82, 1013–1024.

Nelli, F., Bennetts, L.G., Skene, D.M., Monty, J.P., Lee, J.H., Meylan, M.H. and Toffoli, A., 2017. Reflection and transmission of regular water waves by a thin floating plate, *Wave Motion*, 70, 209–221.

Rao, C.P. and Wan, D.C., 2018. Numerical study of the wave-induced slamming force on the elastic plate based on MPS-FEM coupled method, *Journal of Hydrodynamic*, 30(1), 70–78.

Seiffert, B., Hayatdavoodi, M. and Ertekin, R.C., 2014. Experiments and computations of solitary-wave forces on a coastal-bridge deck. Part I: Flat plate, *Coastal Engineering*, 88, 194–209.

Sun, Z., Jiang, Y.C., Zhang, G.Y., Zong, Z., Xing, J.T. and Djidjeli, K., 2019a. Slamming load on trimaran cross section with rigid and flexible arches, *Marine Structures*, 66, 227–241.

Sun, Z., Zhang, G.Y., Zong, Z., Djidjeli, K. and Xing, J.T., 2019b. Numerical analysis of violent hydroelastic problems based on a mixed MPS-mode superposition method, *Ocean Engineering*, 179, 285–297.

Tanaka, M. and Masunaga, T., 2010. Stabilization and smoothing of pressure in MPS method by quasi-compressibility, *Journal of Computational Physics*, 229(11), 4279–4290.

Tang, Z.Y. and Wan, D.C., 2015. Numerical simulation of impinging jet flows by modified MPS method, *Engineering Computations*, 32(4), 1153–1171.

Tang, Z.Y., Zhang, Y.L. and Wan, D.C., 2016. Multi-resolution MPS method for free surface flows, *International Journal of Computational Methods*, 13(4), 1641018.

Wang, X.M., Zhao, X.Z. and Fu, D., 2019. Numerical simulation of water wave interaction with a floating plate breakwater, *The Ocean Engineering*, 37(3), 61–68. (in Chinese)

Zhang, Y.L. and Wan, D.C., 2017. Numerical study of interactions between waves and free rolling body by IMPS method, *Computers & Fluids*, 155, 124–133.

Zhang, Y.X. and Wan, D.C., 2012. Apply MPS method to simulate liquid sloshing in LNG tank, *Proceedings of the 22nd International Offshore and Polar Engineering Conference*, Rhodes, Greece, pp.381−391.

Zhang, Y.X., Tang, Z.Y. and Wan, D.C., 2016. Numerical investigations of waves interacting with free rolling body by modified MPS method, *International Journal of Computational Methods*, 13(4), 1641013.

Zhang, Y.X., Wan, D.C. and Hino, T., 2014. Comparative study of MPS method and level-set method for sloshing flows, *Journal of Hydrodynamics*, 26(4), 577–585.

Zhang, Z.Q., Luan, M.T. and Wang, K., 2013. Flow field analysis of submerged horizontal plate type breakwater, *China Ocean Engineering*, 27(6), 821–828.